Stark Beats in Lyman-Series Emission*

M. J. Alguard† and C. W. Drake‡
Department of Physics, Oregon State University, Corvallis, Oregon 97331
(Received 31 January 1973)

Observed intensity fluctuations in the emission of Stark-perturbed Ly-β radiation, from hydrogen atoms formed by passage of hydrogen ions through carbon foils, are compared with theoretical calculations using a density-matrix formalism to yield information on the cross sections for creation into the various l states. It is found, for beam energies between 250 and 500 keV/atom, that the s states are preferentially populated by more than a factor of 4, compared to a statistical distribution. Similar results are also obtained for Ly-α emission in electric and motional electric fields, in contrast with previous reports at lower energies. The effects of Zeeman splittings, hyperfine interaction, and fringing fields on the signal are investigated.

I. INTRODUCTION

Fluctuations in the intensity of light emitted by foil-excited beams, owing to interference terms in the decay from coherent excited states, have been reported by several authors,[1-11] both under field-free conditions and in the presence of electric or magnetic fields. The beat frequencies serve as a direct measure of the energy splittings of the levels under investigation. In addition, g factors can be obtained,[1,2] and cascade-free lifetime measurements performed,[3] by an analysis of these fluctuations. However, in atoms whose structure is well understood these beats can also serve as a probe of the scattering amplitudes for excitation of the atom into the various possible states as a function of the beam energy.

It has been shown by Macek[12] that under field-free conditions, oscillations in the emitted radiation serve as an indirect measure of the excitation probabilities to the various orbital magnetic (m_l) substates of the configuration under study. Several experimenters have observed these effects.[4-7] With the assumption that an external field can be applied without disturbing the beam-foil interaction, the theory may be extended to include atoms formed in electric or magnetic fields. In addition to the relative initial populations of magnetic substates, information can also be obtained concerning the relative populations of the various l levels for the excited atom. Because of the necessity of doing complicated numerical calculations to obtain these excitation cross sections, previously reported results[8-10] have been qualitative for the most part, or have involved oversimplified models. Below we outline a formulation of the problem in terms of the density matrix that is well suited for computer calculations.

II. THEORY OF QUANTUM BEATS

In the dipole approximation the intensity of emitted radiation for transitions to a group of ground states $|0\rangle$ is given by[13]

$$I^x(t) = K \sum_0 |\langle 0|X|\psi(t)\rangle|^2 , \tag{1}$$

where X is the electric dipole operator, x labels the polarization vector of the emitted radiation, $\psi(t)$ is the excited-state wave function, and K is a constant of proportionality. Inherent in Eq. (1) are the assumptions that any splittings within the ground set $|0\rangle$ or within the excited-state system represented by $\psi(t)$ are small compared to the gross structure involved in the transitions, and that all included transitions fall well within the bandwidth of the detection system. We shall furthermore assume that the excited atomic system $\psi(t)$ is adequately described by the phenomenological theory of radiative damping.[14] Let us select a set of basis states denoted by latin subscripts. The similarity transformation S which diagonalizes the excited-state Hamiltonian will yield the expansion coefficients for the excited eigenstates (denoted by greek subscripts), i.e.,

$$|\alpha\rangle = \sum_k |k\rangle S_{k\alpha} \tag{2}$$

and, inversely,

$$|k\rangle = \sum_\alpha |\alpha\rangle S^{-1}_{\alpha k} . \tag{3}$$

The initial state of the system can also be expanded in the basis set, i.e.,

$$|\psi(0)\rangle = \sum_k a_k |k\rangle . \tag{4}$$

Inserting Eq. (3) into Eq. (4), putting in the explicit time dependence of each eigenstate, and then applying Eq. (2), yields

$$|\psi(t)\rangle = \sum_{k,l,\alpha} |l\rangle S_{l\alpha} S^{-1}_{\alpha k} e^{-i\omega_\alpha t}, \quad (5)$$

where ω_α is the energy eigenvalue, in units of $\hbar$, of the state labeled α. Substituting this last result into Eq. (1) then gives

$$I^x(t) = \sum_{\alpha,\beta} (S^\dagger M^x S)_{\beta\alpha} [S^{-1}\rho(S^{-1})^\dagger]_{\alpha\beta} e^{-i(\omega_\alpha - \omega^*_\beta)t}, \quad (6)$$

where we have defined the monitoring operator[15] M^x by

$$M^x_{jk} = K \sum_0 \langle 0|x|j\rangle^* \langle 0|x|k\rangle, \quad (7)$$

and the initial density matrix ρ by

$$\rho_{jk} = \mathcal{C}_j \mathcal{C}^*_k. \quad (8)$$

It should be noted that since the excited state is described by a phenomenological Hamiltonian (with damping terms), in general, $S^{-1} \neq S^\dagger$ and the eigenvalues ω_α are complex numbers, their imaginary parts being minus one-half the decay constants for the excited eigenstates ($\mathrm{Im}\omega_\alpha = -\frac{1}{2}\gamma_\alpha$).

Inspection of Eq. (6) shows that beats at a frequency corresponding to the energy separation of two eigenstates can occur only if both eigenstates connect to a common ground state via the same dipole operator, and if the system can initially be prepared in a coherent linear combination of these two eigenstates; i.e., both $S^\dagger MS$ and $S^{-1}\rho(S^{-1})^\dagger$ must have off-diagonal elements connecting the two eigenstates.

Suppose, from considerations to be outlined in the next section, that the most general form that ρ can assume is some linear combination of a set of matrices ξ_m, i.e.,

$$\rho = \sum_m \sigma_m \xi_m, \quad (9)$$

where the σ_m's are the expansion coefficients. With this reformulation, Eq. (6) becomes

$$I(t) = \sum_m \sigma_m I_m(t), \quad (10)$$

where I_m is defined by

$$I_m(t) = \sum_{\alpha,\beta} (S^\dagger MS)_{\beta\alpha} [S^{-1}\xi_m(S^{-1})^\dagger]_{\alpha\beta} e^{-i(\omega_\alpha - \omega^*_\beta)t}. \quad (11)$$

The advantage of this reformulation is that the complicated partial intensities $I_m(t)$ depend only upon experimentally known quantities, and can therefore be calculated when the atomic Hamiltonian and the monitoring operator are specified. The experimental unknowns—namely, the expansion coefficients σ_m—can then be determined by a linear fit of the data to the previously calculated partial intensities, i.e., Eq. (10). These expansion coefficients σ_m represent the relative cross sections for excitation of the atom into its various possible states.

III. DENSITY MATRIX

In general, the initial density matrix cannot take on any arbitrary form (subject of course to the constraint $\rho = \rho^\dagger$) but must reflect the symmetry of the interaction which created the atom. In fact, ρ should commute with the entire symmetry group of the beam-foil interaction if the incident beam is unpolarized.

By considering the azimuthal and reflection symmetries of the beam-foil interaction (assuming an amorphous foil), and with the plausible assumption that only electrostatic forces are important during the collision, Macek[12] has shown that the initial density matrix ρ is severely restricted. Since the components of $\vec{L}$, $\vec{S}$, and $\vec{I}$ along the beam axis are separately conserved, ρ has the following form (for one-electron atoms):

$$\langle l', m'_l, m'_s, m'_I | \rho | l, m_l, m_s, m_I \rangle = \sigma(l, l', |m_l|) \delta_{m_l m'_l} \delta_{m_s m'_s} \delta_{m_I m'_I}. \quad (12)$$

Utilizing the completeness relation for the basis set $\{|l, m_l, m_s, m_I\rangle\}$, Eq. (12) becomes

$$\rho = \sum_{l,l',|m_l|} \sigma(l,l',|m_l|) \xi(l,l',|m_l|), \quad (13)$$

where

$$\xi(l,l',|m_l|) = \sum_{\substack{m_s, m_I \\ \text{sign of } m_l}} |l', m_l, m_s, m_I\rangle \langle l, m_l, m_s, m_I|. \quad (14)$$

This expansion of the initial density matrix [Eq. (13)] is just what is desired in Eq. (9), since it takes full advantage of all the known symmetries (i.e., the density matrix has been expressed in terms of as few unknowns as possible).

The expansion matrices $\xi(l,l',|m_l|)$ are of two types; first, those with $l = l'$ that are clearly diagonal and, second, those with $l \neq l'$ that have nondiagonal elements only. In the first case each expansion coefficient $\sigma(l,l,|m_l|) = \sigma_{l|m_l|}$ represents the relative cross section for excitation of the atom into states with the specified $l, |m_l|$. In the second case the expansion coefficients determine the initial coherence between the different l states having the same magnetic quantum numbers.

In the work reported here, we are concerned only with the hydrogen atom in electric fields perpendicular to the beam axis. In such a field the Hamiltonian, and therefore the similarity transformation S, is diagonal in the quantum number $q = (-1)^{l+m_l}$. (This fails when magnetic effects are considered, but we show below that the magnetic field plays a small role in our experiment.) Since the monitoring operator M

is also diagonal in q, the product $S^{\dagger}MS$ is likewise diagonal, and it follows that the right side of Eq. (11) vanishes if α and β correspond to different values of q. Therefore $\xi(l,l',|m_l|)$ can make no contribution to the intensity if l and l' are of opposite parity. Thus for $n=2$ (in hydrogen), only the matrices $\xi_{l|m_l|}$ need be considered, while for $n=3$ the possibility of initial coherence between the s and d states with $m_l=0$ remains. However, these even-parity states contribute to Ly-β radiation only through coupling to the p states via the electrostatic perturbation. Furthermore, the mutual coupling of s and d states is only second order in the applied field. Therefore the contribution of $\xi(s,d,0)$ in Eq. (11) will be small and we neglect it in the following analysis. The remaining six matrices $\xi(l,l,|m_l|)$ are assumed to be sufficient to describe the initial density matrix for Ly-β radiation. It is noteworthy that s-d coherence effects can be important in Balmer series radiation.[6]

IV. MONITORING OPERATOR

The monitoring operator [see Eq. (7)] is determined solely by the geometry of observation and the sensitivity of the detection equipment to polarization. If observation is made in the x-y plane (perpendicular to the beam axis) at an angle ϕ from the x axis, then the net monitoring operator is given by

$$M(\phi)=M^{\varepsilon}+g(M^{x}\sin^2\phi+M^{y}\cos^2\phi), \tag{15}$$

where g is the ratio of detection efficiency for polarization perpendicular to the beam to the efficiency for light polarized parallel to the beam.

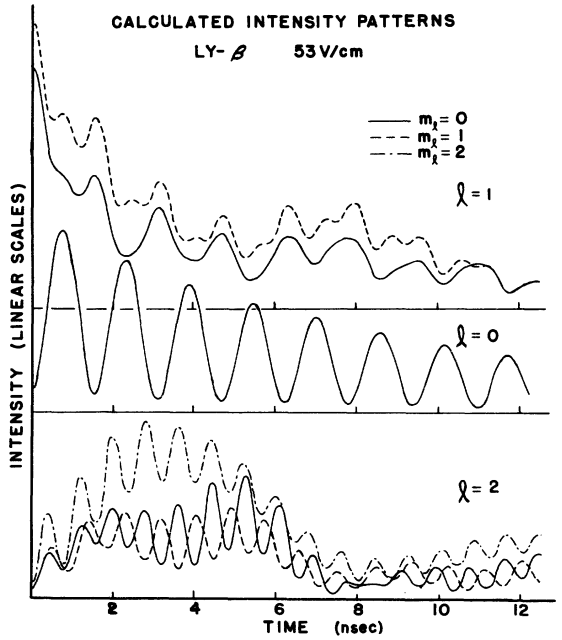

FIG. 1. Partial intensity patterns $I_{l|m_l|}(t)$ for Ly-β in a field of 53 V/cm. The observation axis is perpendicular to the electric field. Hyperfine and magnetic effects are neglected. An averaging over 0.2 nsec is included to approximate our beam sampling function. The $l=2$ curves are exaggerated by a factor of 2.

V. MODEL CALCULATIONS

The Hamiltonian for a hydrogen atom with a specified principal quantum number n in a constant motional electric field is

$$H=H_0+H_{fs}+H_{hfs}+H_S+H_Z+H_R, \tag{16}$$

where H_{fs} and H_{hfs} give the fine and hyperfine structure, respectively, H_S and H_Z are the electric and magnetic perturbations, and H_R is a phenomenological anti-Hermitian damping Hamiltonian representing the free decay rates of the various states involved.[15] When the proper Hamiltonian has been selected, a standard computer routine for solving eigenvalue problems with non-Hermitian matrices gives the similarity transformation S and the complex eigenvalues $\hbar\omega_{\alpha}$. The time dependence of each possible partial intensity $I_{l|m_l|}(t)$ is then obtained directly, using Eq. (11).

For $n=3$ in hydrogen, there are a total of 36 hyperfine states, 34 of which contribute to Ly-β radiation to some degree in an electric field. If, additionally, a magnetic field is present, as in the case with motional electric fields, all states are coupled by the crossed electric and magnetic perturbations, and the number of distinct frequencies in the sum of Eq. (6) or Eq. (11) comes to 342. The computer time necessary to diagonalize the 36×36 non-Hermitian Hamiltonian and to calculate the six partial intensities will be several minutes. Unfortunately, our computing resources did not allow this calculation to be attempted. If, however, hyperfine and magnetic effects can be ignored, the problem reduces to nine states, eight of which are radiative, leaving only 36 frequency terms to consider. With this approximation the six partial intensities can be calculated at moderate cost at any value of the electric field of interest. Figure 1 depicts these six patterns for Ly-β emission with an applied perturbation of 53 V/cm. An averaging over 0.2 nsec is included to approximate the sampling interval of our detection system. Except for magnetic and hyperfine effects, an observed intensity pattern for this field configuration should then be expressible as a linear combination of the six illustrated patterns. The expansion coefficients are the relative cross sections for excitation of

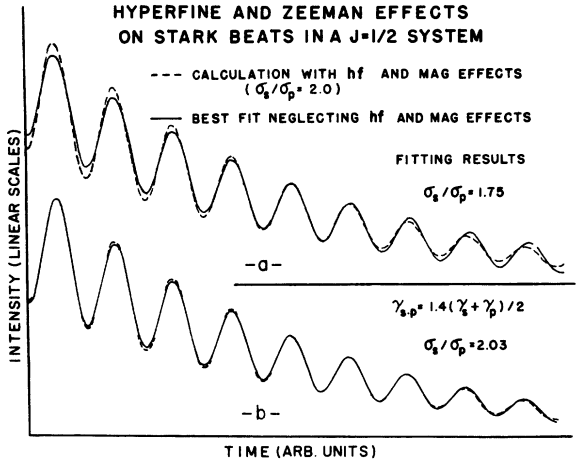

FIG. 2. Hyperfine and Zeeman effects in a $j=\frac{1}{2}$ system with $\sigma_s=2.0\sigma_p$. (a) A best fit of the approximation neglecting hf and magnetic effects to the complete calculation yields $\sigma_s=1.75\sigma_p$. (b) A best fit if the decay rate of the $s_{\frac{1}{2}}-p_{\frac{1}{2}}$ beat is allowed to vary. The cross-section tion ratio $\sigma_s/\sigma_p=2.03$ is in good agreement with the assumed value.

the atom into the six possible sets of states denoted by $l,|m_l|$.

VI. HYPERFINE AND ZEEMAN EFFECTS

The major hyperfine splitting in hydrogen is in the s states. For $n=3$ this splitting is approximately 52.6 MHz. Thus its influence on the data can be expected in times as short as several nanoseconds. Other hyperfine splittings and the Zeeman effect at the magnetic fields we employ are considerably smaller but can nevertheless play a role at longer times. To determine just how much these effects influence the signal, we shall consider an $s_{\frac{1}{2}}$-$p_{\frac{1}{2}}$ (eight-state) system and use the known hyperfine splittings of the $n=3$ levels of hydrogen. Figure 2 shows the results of a complete calculation of the intensity pattern for such a system, including both electric and magnetic interactions, if the initial population of the $s_{\frac{1}{2}}$ level is twice that of the $p_{\frac{1}{2}}$ level. The electric field is 50 V/cm and the magnetic field is 10.0 G, which correspond to typical values in the present experiment. Neglecting the hyperfine and Zeeman splittings, we can make a two-state approximation for the system, calculate the two corresponding partial intensities, and attempt to fit these to the more complete calculation. The results, shown in Fig. 2(a), give an inaccurate determination of the excitation cross sections and a rather poor fit to the "data." Obviously, the major effect of the hyperfine and magnetic interactions is a more rapid attenuation of the beat amplitude than expected, due to the fact that the several frequencies involved between

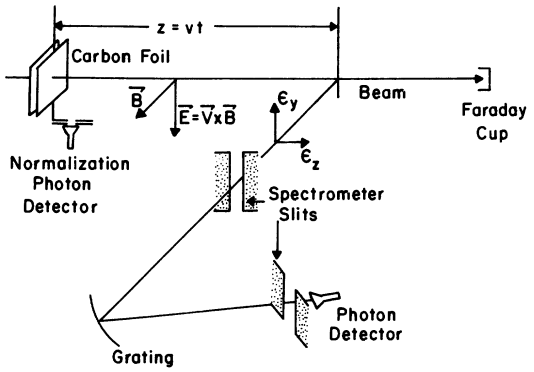

FIG. 3. Schematic diagram of the apparatus. The magnetic field $\vec{B}$ is due to a large coil external to the target region.

$s_{\frac{1}{2}}$ and $p_{\frac{1}{2}}$ states get out of phase as time increases. With an *ad hoc* adjustment of the decay constant of the oscillating term in the two-state calculation, the results shown in Fig. 2(b) are obtained. The cross-section ratio is now within 2% of the correct result and the fit is very good. This procedure is found to be an adequate correction to the model for times less than the period of the dominant hyperfine frequency. Consequently we shall modify the decay factors of any beat-frequency terms for which hyperfine and magnetic effects are important in the calculated intensity patterns. Since a decay time of about 15 nsec represents an upper limit for data taken in this experiment, the only beat term affected will be that corresponding to the $s_{\frac{1}{2}}$-$p_{\frac{1}{2}}$ splitting.

VII. EXPERIMENT

Our beam-foil work is done at the University of Oregon 4-MeV Van de Graaff facility. The ion beam incident on the double carbon foil shown in Fig. 3 is typically H_3^+ with energies in the range of 0.75–1.50 MeV. Energies below this range are not feasible, because of instabilities in the operation of the accelerator below 0.7 MeV. Higher energies, although feasible, have not been investigated, because of a rapid decrease in the cross section for electron capture at the higher beam velocities. Dissociation of the molecules into protons is essentially complete at the first foil. Subsequently, the collision with the second foil results in electron capture by a small fraction of the proton beam. Those hydrogen atoms formed in the $n=2$ or $n=3$ states are the subject of investigation in this experiment. The purpose of two foils, as opposed to one, is to ensure that molecular fragments are well separated when the experiment is begun, at the second foil.[8]

The energy loss of protons in passing through the foil can approximately be taken into account[16];

it results typically in velocity reductions of 1–2%. The uncertainty of this correction can be a fundamental limitation to experiments designed to measure absolute frequency splittings. In the present experiment, since the hydrogen atom is already well understood, the observed beat frequencies are used for final determination of the beam velocity. Velocities thus determined are always found to agree with those predicted from beam energy and foil loss, to within the experimental errors of approximately 1.5%(due primarily to the uncertainty in the motional electric field strength). The spread in particle velocities, owing to straggling or variations in foil thickness, is about 0.5%. This velocity spread will have negligible effect on the data as long as only a relatively small number of spatial beats are observed ($\lesssim$20).

External coils (not shown) produce magnetic fields in the target region of up to 9.0 G, uniform (to within 0.05 G) over a distance of 15 cm, or up to 50 G (for Ly-α measurements), uniform (to within 0.2 G) over about 5 cm. At the beam velocities employed, motional electric fields (in V/cm) are approximately a factor of 10 higher than magnetic fields (in gauss). Usually the field coils are oriented such that the motional electric field is in the vertical direction, as shown in Fig. 3. But for comparison, some data were taken using a horizontal electric field.

For the most part our experimental work was done in motional electric fields, the advantage being that a uniform field over the entire flight path is easily obtained. In earlier work on Ly-α emission, however, Andrä[10] found apparent discrepancies between data taken in purely static electric fields and the equivalent motional fields. In an attempt to repeat this observation, several scans were taken of Ly-α and Ly-β emission, using the assembly diagrammed in Fig. 4 to produce a static electric field perpendicular to the beam.

The signal detection system consists of a 0.5-m Seya-Namioka spectrometer (linear disperson: 16.6 Å/mm) with a bare Channeltron (Bendix model 4028) employed as the photon detector. The entrance and exit slit widths of the spectrometer are typically 1.0 mm. This results in a wavelength resolution of the spectrometer of about 20 Å full width at half-maximum (FWHM), which is sufficient to separate the Ly-α or Ly-β transition from neighboring lines. The beam sampling function was measured by translating a point light source (a focused laser) along the beam axis and measuring the intensity of light reflected from the grating as a function of source position. The measured[4] slit function was nearly triangular, with full width at half-maximum of 0.063 in. Consequently, for the beam velocities typical in our experiment, oscillations with frequencies of somewhat more than 5 GHz can be resolved, with serious attenuation above about 2.5 GHz. For some data the spectrometer slits were opened even further to improve count rates, since it was observed that low frequencies (<1.0 GHz) dominated the signal. The relative selectivity g of the spectrometer for light polarized parallel to the grating rulings, as opposed to light polarized perpendicularly, was previously measured[4] (using the method of Rabinovitch, Canfield, and Madden[17]) to be 3.4 $\pm$0.2 for Ly-β radiation. For Ly-α the same value was assumed.

As in most beam-foil experiments, $I(t)$ is measured by translating the foil upstream from the field of view of the light detector. The known beam velocity then gives the time after formation at which each atom is viewed. It is necessary to monitor the beam in some way to take into account a possible variation of beam parameters with foil position or with time. Therefore, in addition to

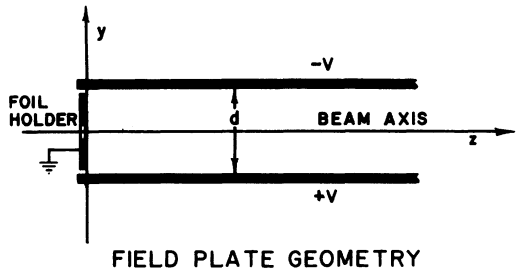

FIG. 4. Electric field plates used to check equivalence of electric and motional electric fields. The plate separation is 1.27 cm.

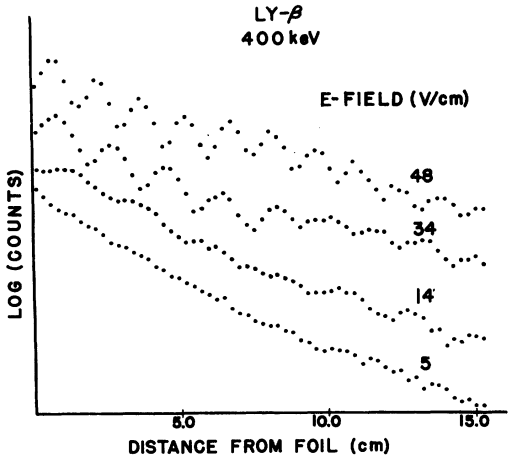

FIG. 5. Signal counts as a function of foil position for several values of the motional electric field.

the actual signal, the following three quantities are sampled for each data point taken: (1) the total ion charge passing through the foil, as measured by counting a digitized integrated Faraday cup current, (2) the time required for each data sample, as determined by counting standard clock pulses, and (3) the number of photons counted by a Channeltron viewing a selected beam segment at a fixed distance from the foil. If normalization of the actual signal is with respect to a fixed integrated Faraday cup current, the clock serves as a measure of accelerator drifts, while the light monitor determines the effect of foil aging on the absolute over-all cross section for excited-state hydrogen formation. We have found for a well-tuned beam and for total scan times of approximately $\frac{1}{2}$ h that all three monitors are constant to within 2%.

All four digitized quantities (consisting of pulses from the Faraday cup integrator/digitizer, a clock, the light monitor, and the actual signal detector) are simultaneously recorded in separate portions of a 4096-channel memory unit (Northern Scientific model NS-630). The addressing logic required is supplied by a locally built unit (utilizing Digital Equipment Corp. M and K series logic modules), which also controls the duration of each data interval by counting a preset number of pulses from a selected input (usually from the integrated Faraday cup current). At the completion of each data sample the address of each signal in the memory unit is automatically incremented by one channel and a pulse train is sent to a stepping motor which increments the foil position a preset distance (any multiple of 0.001 in.). An interlinked PDP-7 computer then allows a preliminary analysis of the data while additional scans are in progress. Finally, the data are punched on paper tape and input into the OSU computing facility for extensive analysis.

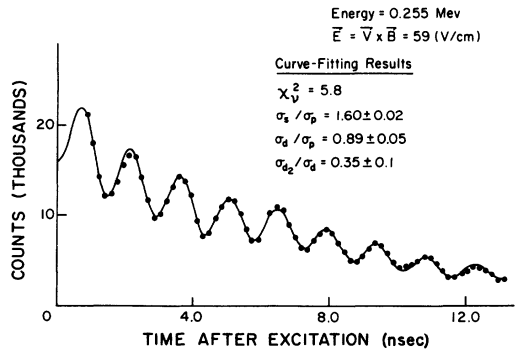

FIG. 6. Curve-fitting results at 255 keV energy in a motional field of 59 V/cm. Uncertainties listed are due to statistics only.

TABLE I. Measured cross-section ratios for beam-foil formation of atomic hydrogen in $n = 2$ and $n = 3$ levels. Since the results of other experimenters are presented in various ways in the literature, conversions to the form presented here were necessary in several cases. Therefore the indicated error factors are only approximately correct.

Energy (keV)	Source	σ_s/σ_p	σ_d/σ_p	σ_{d2}/σ_d
	Statistical expectation	$\frac{1}{3}$	$\frac{5}{3}$	$\frac{1}{5}$
$n=2$				
150	Ref. 9[a]	$<\frac{1}{3}$	•••	•••
200	Ref. 10[a]	0.08(2)	•••	•••
233	Ref. 8[b]	1.45(20)	•••	•••
305	Present study[a]	1.10(10)	•••	•••
340	Present study[a]	1.32(10)	•••	•••
$n=3$				
~100	Ref. 18[c]	1.64(8)	0.69(4)	•••
255	Present study[a]	1.65(15)	0.70(20)	≥0.3
305	Present study[a]	1.30(20)	0.45(15)	•••
340	Present study[a]	1.42(10)	0.59(18)	≥0.3
405	Present study[a]	1.45(10)	0.50(15)	≥0.3
508	Present study[a]	1.42(10)	0.65(15)	≥0.3

[a] Quantum-beats method.
[b] Stark-modified mean lifetime of $n = 2$ levels.
[c] Mean decay rate for H_α radiation in zero field.

VIII. RESULTS

Figure 5 shows data for the Ly-β transition taken at a particle energy of 400 keV for several values of the motional electric field. The frequency resolution of the detection system for these data is approximately 3.5 GHz (for 50% attenua-

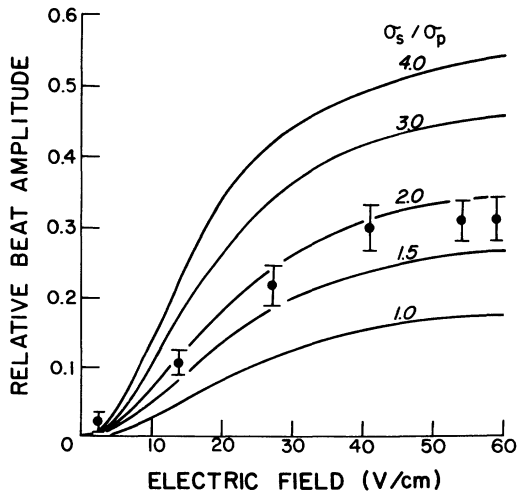

FIG. 7. Calculated relative amplitudes of the $s_{1/2}$-$p_{1/2}$ beat with the assumption $\sigma_{p1} = 1.4\sigma_{p0}$ (Ref. 5). Experimental points are measured amplitudes at 255 keV energy per atom.

tion). It is immediately seen that the Stark-modified Lamb shift produces the dominant beat frequency. Since, to lowest order, the amplitude of this frequency is proportional to the population difference of the $p_{\frac{1}{2}}$ and $s_{\frac{1}{2}}$ levels, we see from the amplitude at $t=0$ that the initial population of the $s_{\frac{1}{2}}$ level is greater than the population of the $p_{\frac{1}{2}}$ level. These observations hold true at all beam energies we have studied.

Figure 6 shows a computer fit to a typical data scan by the method outlined above. Because of the incomplete inclusion of hyperfine and Zeeman effects, the final uncertainties are larger than that determined by statistics alone. In fact, it is found that individual m_l cross sections are usually not well determined, owing to the gross similarity of the partial intensity patterns for a given l but different m_l [see Fig. (1)]. For this reason, the linear combinations $\sigma_d=\sigma_{d0}+2\sigma_{d1}+2_{d2}$ and $\sigma_p=\sigma_{p0}+2_{p1}$ are reported. The three quantities $(\sigma_s, \sigma_p, \sigma_d)$ are proportional to the cross sections for creation into s, p, and d states, respectively. A statistical apportionment would be $\sigma_s:\sigma_p:\sigma_d = 1:3:5$. The initial population of the $p_{\frac{1}{2}}$ level is given by $\sigma_{p_{\frac{1}{2}}}=\frac{1}{3}\sigma_p$. A summary of our results at the particle energies studied is given in Table I. Also listed are results reported by other investigators.

If our model for the calculation is correct, the cross sections determined should be independent of the applied electric field used. Figure 7 shows a family of curves illustrating the variation of beat amplitude with electric field strength (for the $s_{\frac{1}{2}}$-$p_{\frac{1}{2}}$ splitting in the $n=3$ levels) for various values of relative cross sections as calculated from Eq. (10). Also plotted are data points depicting the observed beat amplitudes at various field strengths at a particle energy of 250 keV. These amplitudes are determined by the following procedure: (a) data are smoothed (by successively taking three point averages until the amplitude of the $s_{\frac{1}{2}}$-$p_{\frac{1}{2}}$ beat becomes insignificant), (b) the smoothed data are then subtracted from the original data, and (c) a damped cosine function is fitted to their difference. The amplitude determined for this cosine function approximately represents the amplitude of the $s_{\frac{1}{2}}$-$p_{\frac{1}{2}}$ beat, but the large error bars indicated in Fig. 7 reflect the

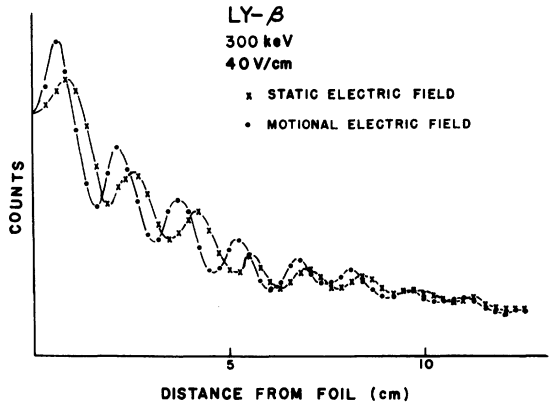

FIG. 9. Comparison of Ly-β data taken in electric and motional electric fields. The phase shift and attenuation of the beats in a static field can be explained by fringing field effects. Curves connecting data points are a visual aid only.

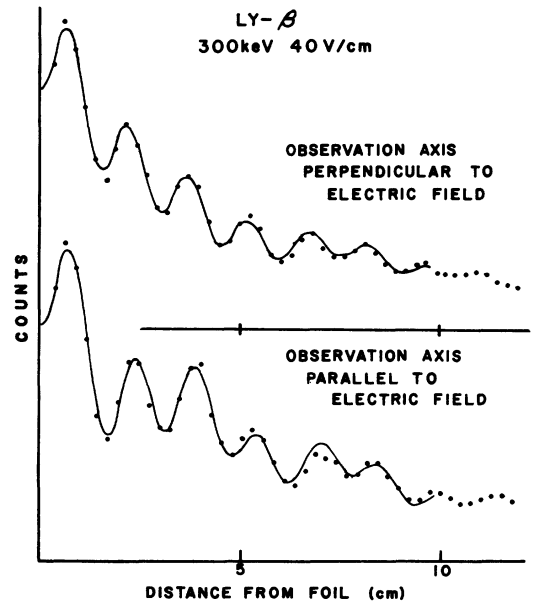

FIG. 8. Effects of direction of observation relative to the induced electric dipole. Beat terms corresponding to $j=\frac{3}{2}$ splittings are much enhanced when observed along the applied field. Solid curves are independent theoretical fits to the two patterns, yielding results consistent to within the statistical errors.

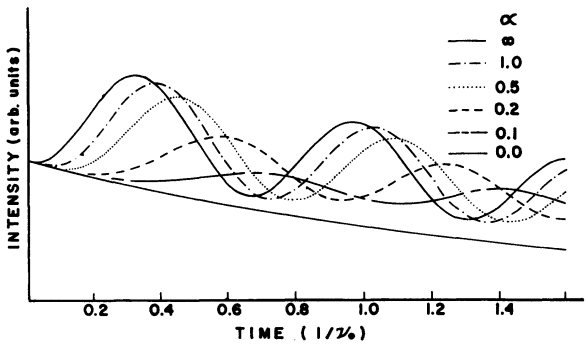

FIG. 10. Calculated effects of fringing field in a $j=\frac{1}{2}$ system at a moderate value of the electric field. The varied parameter is $\alpha=\lambda_0/\pi d$, where λ_0 is the beat wavelength of the unperturbed splitting and d is the separation of the field plates.

fact that the smoothing process affects the data in other ways than just reducing the amplitude of the Lamb-shift beat. The results, however, are consistent with a cross-section ratio $\sigma_s/\sigma_p = 1.75 \pm 0.25$.

Equation (10) can also be used directly to calculate cross sections at each field strength. The results of such calculations are consistent to within the experimental and fitting uncertainties. However, direct application of Eq. (10) becomes less satisfactory as smaller field strengths are considered, for two reasons. First, hyperfine effects become relatively more important than the applied perturbation. Second, at the smaller fields there is less mixing of the s and d states with the p states; therefore the intensity pattern itself contains less information about their relative populations.

The intensity pattern is also dependent upon the azimuthal direction of observation relative to the electric field axis, since the monitoring operator is a function of this direction [Eq. (15)]. Figure 8 is a comparison of data taken in an electric field parallel to the direction of observation with data taken in a similar field perpendicular to this axis. It is observed that the relatively-low-frequency terms corresponding to the $j = \frac{3}{2}$ splittings are greatly enhanced when observed along the induced dipole moment. Also shown in Fig. 8 are the theoretical fits to the two intensity patterns. The fact that the independent fits yield equivalent results for the cross sections (within the statistical errors) best illustrates that the formalism employed does predict the observed azimuthal dependence of the intensity pattern.

Figure 9 is a comparison of Ly-β intensity patterns taken in motional electric and equivalent electrostatic fields. The electric field geometry is pictured in Fig. 4. The electric field beats appear to be attenuated and phase shifted with respect to the data taken in an equivalent motional electric field. Since the theory developed here assumes a time-independent Hamiltonian (the external fields are present at $t = 0$ and constant), the apparent discrepancy is probably due to the effects of fringing field in the pure electric field case. To test this hypothesis, we again resort to a $s_{\frac{1}{2}}$-$p_{\frac{1}{2}}$ system, which is simple enough to allow a complete (numerical) calculation of the fringing field effects.

The field geometry (Fig. 4) can be solved in closed form (with the assumption that the gap between either field plate and the foil holder is much less than the plate separation). The result is

$$E_y = \frac{2V}{d} \frac{1 - r^2}{D} \tag{17}$$

and

$$E_z = -\frac{4V}{d} \frac{r \sin(2\pi y/d)}{D}, \tag{18}$$

where $r = e^{-2\pi z/d}$ and $D = 1 + 2r\cos(2\pi y/d) + r^2$. The set of coupled differential equations $[\dot{\rho}(t) = -i\hbar(H\rho - \rho H^{\dagger})]$ describing the wave function of a four-state $(s_{\frac{1}{2}}, \pm\frac{1}{2}; p_{\frac{1}{2}}, \pm\frac{1}{2})$ system, entering such a field with constant velocity in the z direction, can be numerically integrated by standard techniques. Figure 10 shows the results of such a calculation for $y = 0$ in a nominal electric field $(E = 2V/d)$ for which the nonvanishing matrix elements of the perturbation Hamiltonian are equal to 0.6 times the energy separation of the unperturbed levels. In general, the beat is seen to be attenuated and phase shifted with respect to the sudden approximation, as expected. The magnitude of the effect is best parametrized by the quantity $\alpha = \lambda_0/\pi d$, where λ_0 labels the beat wavelength of the unperturbed energy separation. For $\alpha > 2.0$ the sudden approximation becomes valid, while for $\alpha < 1.0$ serious attenuation of the beat results. Off axis $(y \neq 0)$, similar results are obtained, except that the beat is never completely attenuated, since some field always exists at the foil $(z = 0)$. In the present experiment our beam is confined to the region $|y| \leq \frac{1}{8}d$, a region for which the solution for $y = 0$ is adequate. For the data shown in Fig. 9, $d = 1.27$ cm and $\lambda_0 = 2.5$ cm. Therefore $\alpha \simeq 0.6$, and we expect from Fig. 10 approximately a 25% reduction in beat amplitude and a phase shift of 60°. The observation (Fig. 9) agrees quite well with this prediction, considering that the contribution of $j = \frac{3}{2}$ and $j = \frac{5}{2}$ levels has been ignored. For Ly-α the effect is more serious. In this case $\alpha \simeq 0.2$, and Fig. 10 predicts a 140° phase shift and a 50% amplitude reduction. Again the observed results are in good qualitative agreement. Our conclusion is that electrostatic fields yield intensity patterns equivalent to their corresponding motional electric fields when fringing effects are taken into account. Consequently, we suggest that the effects of fringing fields may account for a failure in previous experiments[10,11] to observe Stark beats in electrostatic fields perpendicular to the beam axis.

Figure 11 shows Ly-α data taken at 310 keV in a motional electric field. The observed beat minimum at the foil indicates $\sigma_s > \sigma_{p_{\frac{1}{2}}}$ (the computer fit yields $\sigma_s = 3.3\sigma_{p_{\frac{1}{2}}}$), in marked contrast to results reported by Sellin *et al.*[9] and Andrä,[10] at 150 and 200 keV, respectively. We agree, however, with the results of Bickel,[8] obtained at 238 keV by measuring the contribution of the s states to the decay rate of the Ly-α radiation. All of these results are consistent with a large

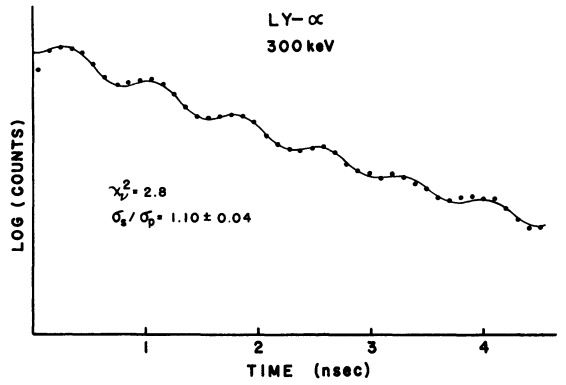

FIG. 11. Ly-α beats in a motional field of 200 V/cm. The solid curve is a theoretical fit to the data showing that s levels are preferentially populated by a factor of 3.3 compared to a statistical distribution.

variation in initial-state populations with beam energy. However, the mechanism behind such a dependence of the relative cross sections on beam energy is unclear at this time. Also we have observed the $n = 3$ relative cross sections to be approximately constant over the energy range 250–500 keV.

An alternative explanation could involve the individual field geometries used. Andrã[10] employed an electric field parallel to the beam axis by using the foil holder as one field plate. In a parallel field it is possible that the effects of initial coherence between the s and p states could be observed (see Sec. III). It is doubtful that a large reversal of beat amplitude would result from such effects, although Andrã attributed his failure to see beats in a crossed electric field to coherence, but with alignment perpendicular to the beam axis rather than along it.

IX. CONCLUSIONS

We have employed a theoretical calculation of the expected intensity patterns for Ly-α and Ly-β emission in a suddenly applied constant-motional electric field to measure relative cross sections for excitation of the atoms into the various l states for the $n = 2$ and $n = 3$ shells. The calculation is found to be in good quantitative agreement with the observed dependence of the intensity pattern upon the strength and direction of an applied electric field.

The major effects of the hyperfine and Zeeman interaction on the intensity pattern were predicted by consideration of a $j = \frac{1}{2}$ system and are found to account adequately for the observed rapid attenuation of the Lamb-shift beat frequency. Ly-α and Ly-β data in a static electric field provided by condenser plates are found to be in good qualitative agreement with those taken in a motional electric field, providing fringing field effects are taken into account. We therefore suggest that the apparent discrepancy reported by Andrã[10] between Ly-α beat amplitudes found in pure and motional electric fields may be due to fringing fields, rather than magnetic effects, which were shown above to play a small role.

Finally, we found strong preferential population of the s states for both the $n = 2$ and $n = 3$ levels at the observed beam energies. This result, when compared with previous observations[9,10] of preferential population of p states at lower energies, suggests either a strong variation of cross-section ratios with beam energy or initial coherence between the s and p states. An alternative explanation could be that the relative cross sections are sensitive to the particular foil used. Additional measurements, especially below 250 keV, may shed light on this subject.

ACKNOWLEDGMENTS

The support and hospitality of the Nuclear Physics Group at the University of Oregon is gratefully acknowledged. The authors also extend their appreciation to Professor C. E. Fairchild for several useful suggestions and for his continued interest in this experiment, and also to Dr. Charles E. Johnson for his assistance and encouragement during his stay here.

*Work supported in part by a Cottrell Grant from the Research Corporation to C.W.D. and by the National Science Foundation through the Nuclear Physics Group at the University of Oregon.

†Present address: Gibbs Laboratory, Yale University, New Haven, Conn.

‡On sabbatical leave for 1972-73 at the Clarendon Laboratory of Physics, Oxford University, England.

[1]C. H. Liu, S. Bashkin, W. S. Bickel, and T. Hadeishi, Phys. Rev. Lett. **26**, 222 (1971).

[2]C. H. Liu and D. A. Church, Phys. Lett. **35**, 407 (1971).

[3]C. H. Liu and D. A. Church, Phys. Rev. Lett. **29**, 1208 (1972).

[4]D. J. Lynch, C. W. Drake, M. J. Alguard, and C. E. Fairchild, Phys. Rev. Lett. **26**, 1211 (1971); also D. J. Lynch, Ph.D. thesis (Oregon State University, 1972) (unpublished).

[5]H. J. Andrä, Phys. Rev. Lett. **25**, 325 (1970).

[6]D. J. Burns and W. H. Hancock, Phys. Rev. Lett. **27**, 370 (1971).

[7]H. G. Berry and J. L. Subtil, Phys. Rev. Lett. **27**, 1103 (1971).

[8]W. S. Bickel, J. Opt. Soc. Am. **58**, 219 (1968).

[9]I. A. Sellin, C. D. Moak, P. M. Griffin, and J. A. Biggerstaff, Phys. Rev. **184**, 56 (1969); also Phys. Rev. **188**, 217 (1969).
[10]H. J. Andrä, Phys. Rev. A **2**, 2200 (1970); also Nucl. Instrum. Methods **90**, 343 (1970).
[11]E. H. Pinnington, H. G. Berry, J. Desesquelles, and J. L. Subtil, Nucl. Instrum. Methods **110** (to be published).
[12]J. Macek, Phys. Rev. A **1**, 618 (1970).
[13]J. P. Barrat, J. Phys. Radium **20**, 541 (1959); J. Phys. Radium **20**, 633 (1959); P. R. Franken, Phys. Rev. **121**, 508 (1961); also G. W. Series, Phys. Rev. **136**, 684 (1964). This equation is a straightforward generalization of the expression for the electric dipole transition probability found in any standard textbook. For example: H. Bethe and E. Salpeter, *Quantum Mechanics of One- and Two-Electron Atoms* (Academic, New York, 1957), pp. 248 and 249.
[14]E. Wigner and V. Weisskopf, Z. Phys. **63**, 54 (1930); also W. E. Lamb, Jr. and R. C. Retherford, Phys. Rev. **79**, 549 (1950).
[15]For a discussion of the monitoring operator see, for example, T. R. Carver and R. B. Partridge, Am. J. Phys. **34**, 339 (1966).
[16]L. C. Northcliffe, Annu. Rev. Nucl. Sci. 13, 16 (1963).
[17]K. Rabinovitch, L. R. Canfield, and R. P. Madden, Appl. Opt. **4**, 1005 (1965).
[18]H. H. Bukow, H. V. Buttlar, D. Hass, P. H. Heckmann, M. Hall, W. Schlagheck, D. Schurman, R. Tielert, and R. Woodruff, Nucl. Instrum. Methods **110** (to be published).

PHYSICAL REVIEW A VOLUME 8, NUMBER 1 JULY 1973

Lamb Shifts in Two-Electron Atoms

H. G. Berry* and R. Bacis
Laboratoire de Spectrométrie Ionique et Moléculaire (associé au CNRS), Université de Lyon I, 43 bd du 11 nov 1918, 69 - Villeurbanne, France
(Received 20 November 1973)

From an absolute wavelength measurement of the $2s\,^3S_1$-$2p\,^3P_1$ transition in ^{7}Li II we deduce a Lamb shift of 1.274 ± 0.015 cm^{-1}, compared with a theoretical value of 0.99 ± 0.04 cm^{-1} for the $2s\,^3S_1$ level. We suggest that the difference is due to a Lamb shift of the $2p\,^3P_1$ level and show that other measurements in isoelectronic two-electron spectra are in accord with this prediction.

INTRODUCTION

Measurements of Lamb shifts in two-electron atoms are difficult to make, primarily because the nondegeneracy of the ns, np excited states prohibits the applicability of microwave techniques. The principal existing measurements are by Herzberg[1] in He I and by Edlén and Löfstrand[2] in C V which have accuracies of about 10%. A summary of these measurements has been given by Accad *et al.*[3] The only accurate calculations of Lamb shifts in excited states of two-electron atoms are by Suh and Zaidi[4] for the $2s\,^{1,3}S$ states in He I. The recent calculations of the energies of such states by Accad *et al.*[3] include relativistic effects but exclude radiative corrections. Hence, through a direct energy-difference measurement, we can derive the differential Lamb shift of the two states involved. The best examples of such transitions are the $ns\,^{1,3}S$-$n'p\,^{1,3}P$ transitions with $n=n'$, where the Lamb shifts remain a significant fraction of the total energy difference. We shall describe an accurate measurement of the Lamb shift in such a transition with $n=2$ in ^{7}Li II, and compare our result with existing data in other two-electron atoms.

EXPERIMENT

The ^{7}Li II transition $2s\,^3S - 2p\,^3P$ at 5485 Å was excited in a liquid-nitrogen-cooled double-anode hollow cathode and observed in high resolution with a HYPEAC[5] spectrometer. The cathode walls were "dressed" with different compounds[6] (Li, Li_2CO_3, LiOH). The grating premonochromator was centered on, and transmitted light of, a single Fabry-Perot fringe, the two systems being scanned synchronously in wave number. A second Fabry-Perot, in parallel with the first, provided calibration fringes which were compared with a thorium standard source for the absolute wavelength measurements. Optically contacted spectrosil spacers ensured the necessary stability. Since the $2p\,^3P$ term of Li II is more than 65 V above the neutral lithium ground state, the excitation is very weak and the consequent light intensity is low. In addition, the transition is very wide (6.5 cm^{-1}), due to fine and hyperfine structures, and a single scan took approximately 12 h. The stability of the spectrometer, which was in a temperature-controlled box, was checked with the calibration fringes, compared to thorium spectra.

In this first work the absolute wavelength accu-